International Journal of Technology 14(3) 628-637 (2023)
Received September 2021 / Revised October 2021 / Accepted December 2021

International Journal of Technology

http://ijtech.eng.ui.ac.id

Effect of Pressure on Salt Water Spray as Alternative Methods of Desalination Using Droplet Evaporation-Air Entrainment

Muhamad Agil Fadhel Kurnianto[1], Ridho Irwansyah[1], Leonardo Fabianto[1], Arya Armadani[1], Warjito[1*]

[1]*Department of Mechanical Engineering, Faculty of Engineering, Universitas Indonesia, Kampus UI Depok, Depok 16424, Indonesia*

Abstract. It is necessary to utilize desalination technology to clear the water available, including seawater, to meet the increasing need for clean water due to population growth. Several desalination methods, such as thermal methods, membranes, freezing g, and ion exchange, continue to be developed but have not overcome some deficiencies. Therefore, new alternative desalination methods with droplet atomization, which utilizes the air entrainment phenomena, are being developed. Research on non-dimensional fluid atomization is the basis for designing this method. The study used brine pumped through a nozzle with a small diameter to become mist or vapor. This study carried out variations of research parameters on the configuration of the experimental apparatus in the form of pressure, the diameter of the nozzle, and the number of nozzles. Quantitative data from experimental results obtained from measurement instruments and qualitative data in videos obtained using a camera are to be processed into quantitative data using image processing. The results showed that pressure affects the characteristics of a full cone-shaped water spray. It was found that the best spray system configuration with two nozzles with a diameter of 0.5 mm in a pressure of 9 bar.

Keywords: Desalination; Droplet; Non-dimensional; Pressure; Water spray characteristics

1. Introduction

In Indonesia, the threat of lack of clean water every year always increases and ranks 51st with a high level of crisis risk (40 to 80%) (Statistik, 2020). Indonesia has a coastline of 81,000 kilometers and a sea area of about 5.8 million square kilometers. Thus, Indonesia can take advantage of abundant seawater as an alternative to meet the deficit in clean water needs for the community with desalination technology.

The utilization of desalination technology is one of the options in processing abundant natural seawater resources. However, one of the challenges facing all desalination technologies is high energy consumption. Various efforts have been made, one of which is by integrating multiple renewable energy sources into existing desalination technology, including RO/PV (photovoltaic) plants (Arunkumar *et al.*, 2013), solar thermal generators/MED (Chen, Li and Chua, 2016), geothermal-based MED plants (Chen *et al.*, 2016), combined CSP (solar power plant) and desalination plant (MED or MSF) for the

*Corresponding author's email: warjito@eng.ui.ac.id, Tel.: +62 812-1997-2970
doi: 10.14716/ijtech.v14i3.5153

cogeneration of electricity and freshwater (Chen *et al.*, 2019; Christ, Regenauer-Lieb and Chua, 2014; Darwish *et al.*, 2012) .

There are also solar-powered humidification-dehumidification (HDH) desalination systems (El-Fiqi *et al.*, 2007) and industrial waste heat (Gude, 2011), and solar-driven membrane distillation (He *et al.*, 2015). (Kusuma, Putra and Respati, 2018) study modified the existing desalination system by adding thermosyphons. The results show that the use of thermosyphons in cascade solar desalination systems can increase the efficiency of the thermal system up to 2.35 times. Research technology using microbial technology is also carried out (Utami, Arbianti and Manaf, 2015). The results obtained can remove the salt content of about 55.03%.

Desalination technology with a low-temperature spray method applying direct contact heat and mass transfer mechanism is one of the new technologies. Compared to traditional thermal desalination technology, spray-assisted low-temperature desalination has the key benefits of high heat and mass transfer rates, simplicity of system design, scaling, and lower initial costs (Abdelkareem, 2019). There are several studies related to experimental studies have been carried out regarding the evaluation of its thermal performance (Wellmann *et al.*, 2015; El-Agouz, Abd El-Aziz and Awad, 2014; Miyatake *et al.*, 1981a; Miyatake *et al.*, 1981b) on flash spray evaporation to increase the evaporation rate, investigated the impact of design (nozzle) and operating parameters (injection direction) (Mutair and Ikegami, 2008), initial liquid temperature, spray velocity, and degree of superheat (El-Fiqi *et al.*, 2007), and evaluate its application in renewable energy utilization and waste heat recovery. Analytical studies have also been carried out to model the equations of heat and mass transfer processes in the spray evaporator (Hwang and Moallemi, 1988) and were carried out to investigate the thermal performance of the entire system (Mutair and Ikegami, 2009; Miyatake *et al.*, 1981b). In the study, experimented with the evaporation of flash spray in a jet of superheated water introduced into a low-pressure chamber. The feed temperature varied from 40 °C to 80 °C. Based on these experiments, empirical equations were obtained to predict distillate production. In another study (Ikegami *et al.*, 2006) experimented with comparing opposite injection directions, i.e., up and down jets, on the performance of a desalination spray for superheated conditions. It was found that the flash evaporation process worked better but with a shorter distance towards the top. (Mutair and Ikegami, 2009) conducted a similar study on flash evaporation using an upward jet with a larger nozzle. They found that the intensity of flash evaporation increased with higher initial water temperature and degrees of superheat.

The study of (Chen *et al.*, 2016) carried out a simulation process on the droplet evaporation process in a single-stage configuration to observed the relationship between increased water productivity and initial droplet velocity. Furthermore, Chen and coworkers (Chen, Li and Chua, 2016) also conducted a simulation study on a multi-stage direct contact spray evaporation and condensation system. Based on the results of the study of water production and thermal efficiency for several stages, there was a significant increase compared to the single-stage system.

From the literature review above, an important parameter governing the evaporation method of seawater desalination sprays is the need for an optimal design of the water droplet size for the evaporation process. Until now, research on the characterization of spray evaporators has not been comprehensively studied, although it is an important parameter in droplet formation. This study discusses the effect of non-dimensional parameters on spray as a first step in developing and identifying the hydrodynamic aspects of droplets because these characteristics have not been discussed fundamentally. Non-dimensional parameters commonly used in fluid mechanics include the Reynolds number,

Mach number, Froude number, and Weber number are used in geometric scaling and develop dynamic similarities to the experimental process. This research is intended to conduct laboratory-scale experiments to create a new desalination technology system that can purify seawater. This research was conducted to artificial seawater by making a saltwater solution by taking into account the variables of nozzle diameter (Dn), the number of nozzles (n), and pressure (P) as factors that influence the occurrence of droplets. Thus, it is possible to know the phenomena of the characteristics of the droplet spray or saltwater droplets to produce clean water.

2. Methods

2.1. Analytical Review

Several factors influence droplet formation: flow pressure, spray pattern, spray angle, nozzle type, fluid-specific gravity, fluid viscosity, and surface tension. Some of these parameters influence different tendencies from each other. In the analysis, each of these factors can be used as a similarity relationship. The general similarity equation for droplet size with the comparison of the size and fluid parameters of water. Pressure and droplet size have an inverse relationship; the higher the fluid pressure that passes through the nozzle, the smaller the droplet size formed. This relationship is formulated as follows:

$$\frac{D_1}{D_2} = \left(\frac{P_1}{P_2}\right)^{-0.3} \tag{1}$$

Which, D = Diameter (m), P = Pressure (Pa)

The non-dimensional number is a parameter used to determine fluid flow characteristics in an experimental system (Rapp, 2016). There are several non-dimensional numbers, including the Reynolds number, which is a number that is used as a marker of a flow that is categorized as turbulent flow and laminar flow. The Reynolds number is the ratio between the inertial and viscous forces (Uruba, 2018). This Reynolds equation is expressed in the following form (Rapp, 2016):

$$Re = \frac{Inertia\ Force}{Viscous\ Force} = \frac{\rho\ v\ D}{\mu} \tag{2}$$

Which, Re = Reynolds number, ρ = density of fluid (kg/m^3) v = velocity of fluid (m/s), D = diameter (m), μ = Absolut viscosity (kg/m s)

A Froude number is a non-dimensional number that serves as a parameter to determine whether a flow will follow downstream or upstream (Mayer and Fringer, 2017). In general, the value of the Froude number is a comparison between the inertial force and the gravitational force acting on the system (Rapp, 2016);

$$Fr = \sqrt{\frac{Inertia\ Force}{Gravity\ Force}} = \frac{v}{\sqrt{Dg}} \tag{3}$$

Which, Fr= Froud Number, v = velocity of fluid (m/s), D = diameter (m), g = gravitation (m/s^2)

The Weber number is a non-dimensional number that shows the properties shown by the flow of a fluid turning into a droplet (Rapp, 2016). The characteristics of the spray nozzle can be determined using the Weber number. The deformation force referred to in the calculation of the Weber number is the aerodynamic force, expressed in the following form (Rapp, 2016).

$$F_A = \frac{CW\pi D^2 \rho v^2}{8} \quad (4)$$

Meanwhile, the force that resists or opposes the deformation caused by aerodynamic forces is called the cohesive force. The value of this force depends on the surface tension of the fluid itself and its surface. This style is expressed as follows (Rapp, 2016);

$$F_K = \pi D\ \sigma \quad (5)$$

Which, F_K = Deformation Force, D = diameter (m), σ = surface tension (N/m)
Weber numbers are expressed in the following equation (Rapp, 2016);

$$We = \frac{Inertia\ Force}{Surface\ Force} = \frac{v}{\sqrt{\sigma/\rho D}} \quad (6)$$

Which, We = Bilangan Weber, ρ = density of fluid (kg/m^3), v = velocity of fluid (m/s), D = diameter (m), σ = surface tension (N/m)

2.2. Experiment Design

In this study, the experimental apparatus was assembled as several components, as shown in Figure 1. The flow process is described in the Process Flow Diagram (PFD), that a seawater pump circulates the salt flow to the nozzle. In this study, the manufacture of salt water was carried out by mixing the composition of water and salt solution to meet the 20000 ppm salinity standard, which is the minimum ppm standard for seawater (Nugroho, 2004). Measurement of salt content in this study was measured using a refractometer. The nozzle's output is a droplet directed to move through the transportation pipe to the condensate container. In a series of transportation pipelines, blowers are used to assist the flow.

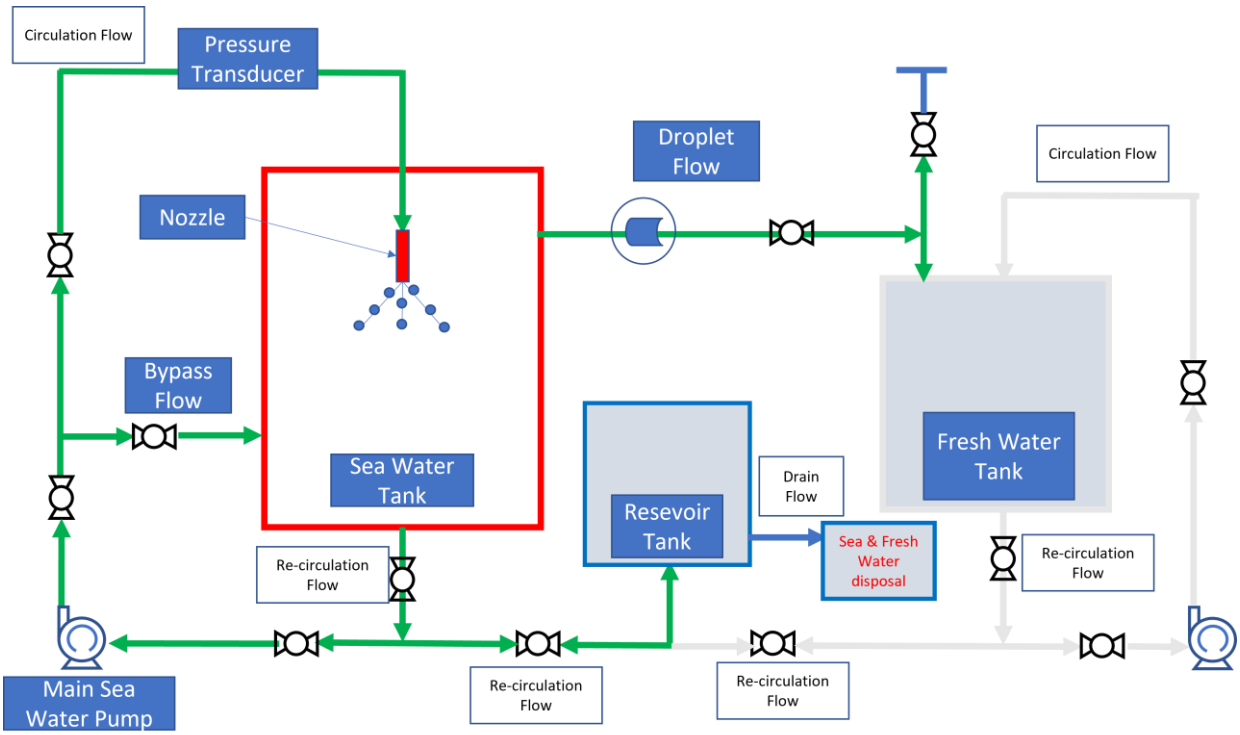

Figure 1 Process Flow Diagram (PFD)

In this study, the limitations of the evaporator room under investigation were carried out, as shown in the flow diagram for the green color. In this study, several nozzle

configurations were carried out related to the nozzle It can be seen in Figure 2 that the misting nozzle used is a nozzle with a diameter of 0.2-0.5 mm for the variation of the data studied. This Misting Nozzle serves to remove salt solution water droplets. Table 1 shows the nozzle configuration used in this experiment formation: flow pressure, spray pattern, spray angle, nozzle type, fluid specific gravity, fluid viscosity, and surface tension. Some of these parameters influence different tendencies from each other. In the analysis, each of these factors can be used as a similarity relationship. The general similarity equation for droplet size with the comparison of the size and fluid parameters of water.

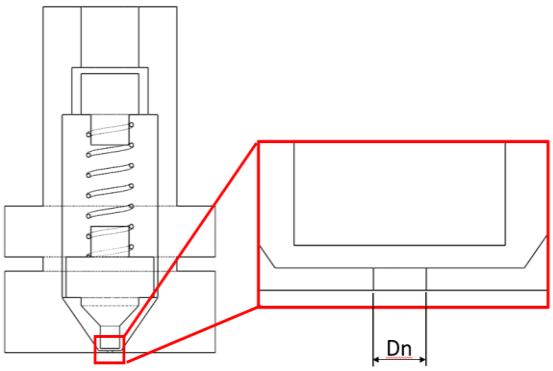

Figure 2 Nozzel Configuration for Diameter nozzle variation (Dn)

Table 1 Variation of experiment

Parameter	Misting Nozzle Various
Diameter Nozzle	0.2 mm, 0. 3 mm, 0.4 mm, 0.5 mm
Number of Nozzles	1 nozzle, 2 nozzle, 4 nozzle
Pressure Variation	7 Bar, 8 Bar, 9 Bar, 10 Bar

2.3. Experiment Procedure

The experiment was carried out by varying the water pressure in the pipe leading to the nozzle with a nozzle configuration of both diameter and number. This study was carried out by opening/closing the valve until it reached a pressure that was varied as a control parameter in this study. Water pressure is varied 6 bar, 7 bar, 8 bar, 9 bar.

Data were collected by observing and measuring the parameters related to the process of forming saltwater droplets. Figure 3 Observation evaporator chamber made using acrylic material with dimensions of 600 mm long, 600 mm wide, and 800 mm high. In this observation case, images will be taken using a Nikon D5200 camera with a frame rate of 50 images per second (fps), as shown in Figure 3. to capture the process of forming saltwater droplets.

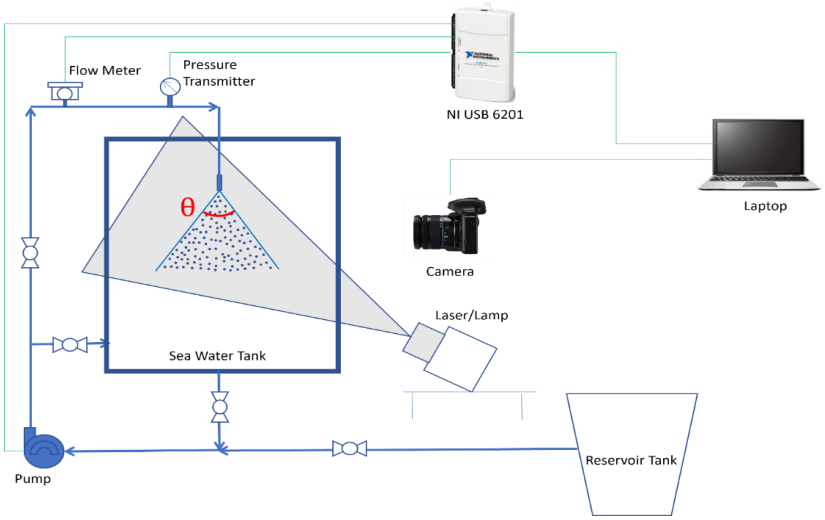

Figure 3 Experiment setup and apparatus

To obtain data as accurately as possible, the author uses a data processing application (image processing), namely the 'Image J' software, which is an image processing software. The software can filter images by 2048 x 2048 pixels in just 0.1 second, 8-32 bit in RGB color in wide format. Image J offers image enhancement as an option due to the need for high-speed photo capture (Warjito, Harinaldi and Setyantono, 2016). The use of "Image J" is useful for obtaining the value of the spray angle, as shown in Figure 3.

3. Results and Discussion

3.1. Droplet Formation

The droplet phenomenon was recorded and then processed to obtain qualitative data. The recorded data is then processed using software to get quantitative data. As illustrated in Figure 4, the water spray received from the visual data processing in this study is a full cone spray so that each structural segment can be identified as in Figure 4(a) and compared with the schematic of the spray cone angle structure in Figure 4(b). Water spray pattern and angle are important factors in droplet characteristics and formation. In the results of the study, which were compared with the study (Zhang *et al.*, 2015), the droplet characteristics were formed into several regions. These include the Potential core region, the main region, and the diffused droplet region. This potential core region shows irrotational movement. In the Main Region, the jet axial velocity and dynamic pressure decrease gradually with strong turbulent characteristics. Meanwhile, in the Diffused Droplet region, there is a mixture of the jet medium and the environment with relatively low axial velocity and dynamic pressure, so the jet loses cohesion.

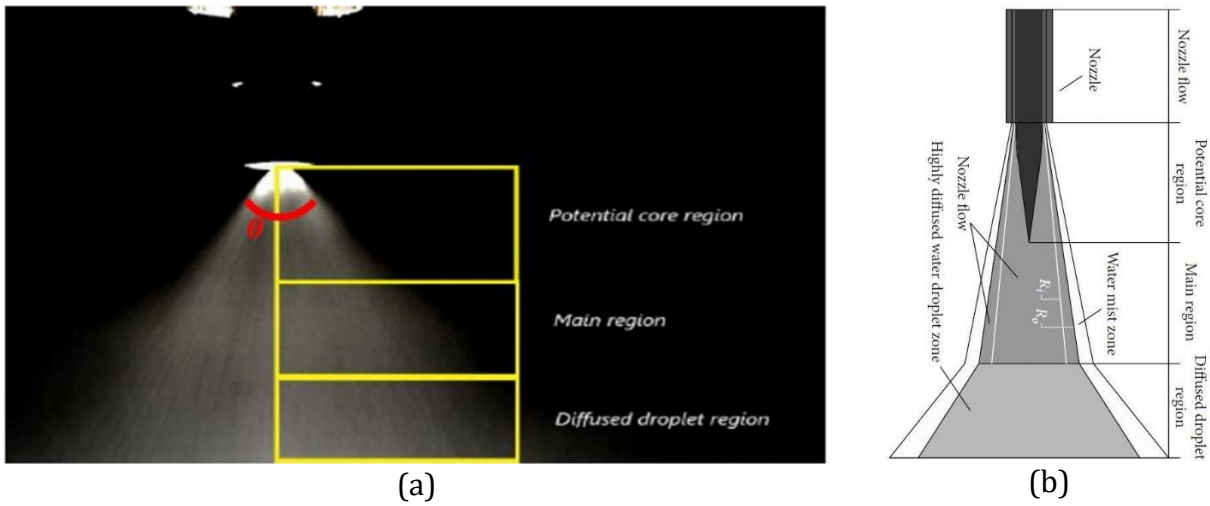

(a) (b)

Figure 4 Dispersion Zone Division of the resulting Droplets based on (a) Experimental Results and (b) Jet Modeling Theory.

3.2. Effect of Water Pressure on Water Spray Angle

In Figure 5 which shows a graph of the effect of water pressure on the water spray angle, it can be seen that the water spray angle increases with each increase in pressure and nozzle diameter. Significant changes in the angle of the water spray occur in the double nozzle and the diameter of 0.5 mm. At the time of the study, using a double nozzle and a diameter of 0.5 mm produced the largest spray angle at a pressure of 9 bar.

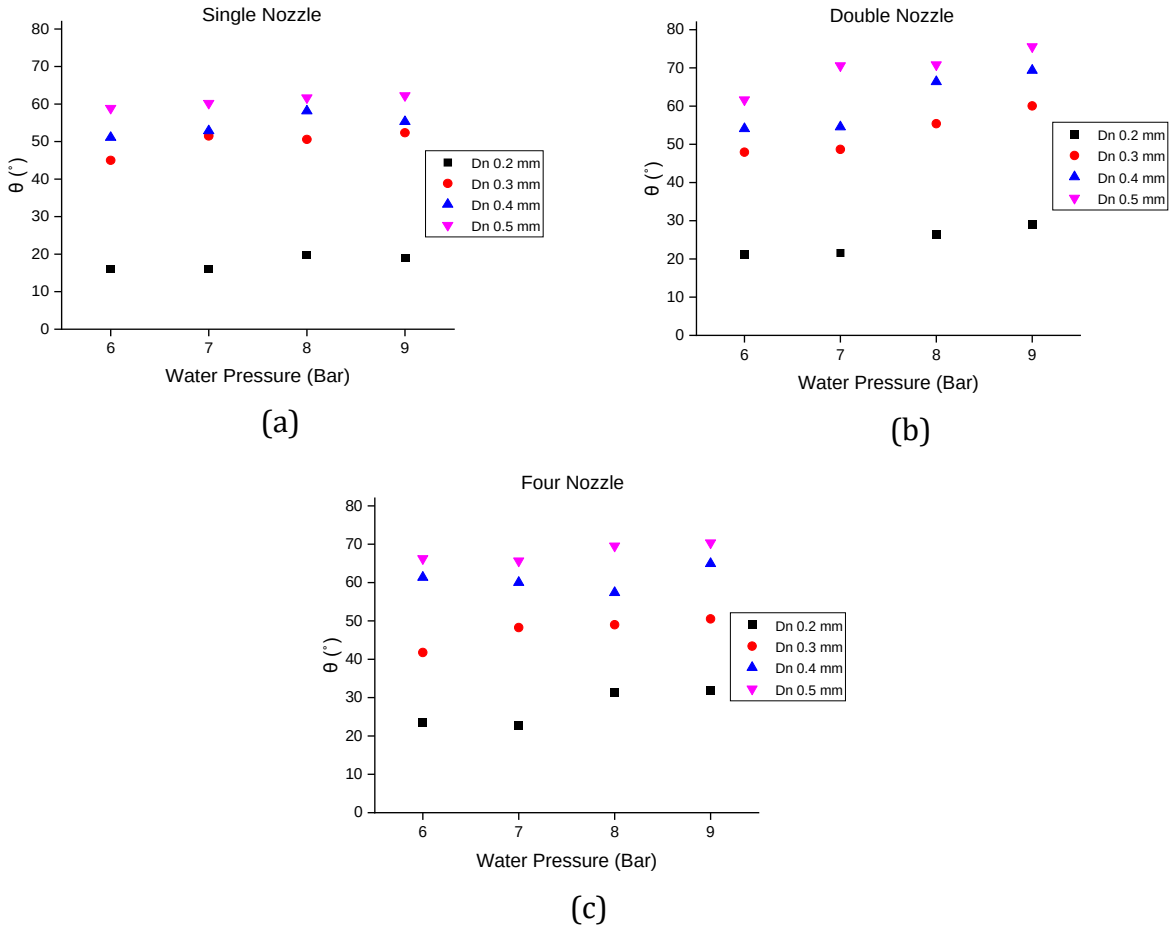

Figure 5 Graph of the effect of water pressure on the angle of water spray with variations in nozzle diameter and several numbers of the nozzle (Pp vs. θ) on (a) single nozzle, (b) double nozzle, (c) four nozzle

The change in spray angle occurs because the nozzle lowers the fluid pressure, which influences the droplet diameter so that the main and diffuse droplet areas expand when the pressure entering the nozzle increases. While the enlarged nozzle diameter will cause the spray diameter to increase. In this case, the water spray angle will also increase. A wider spray angle increases the atomization rate of the liquid and reduces the droplet size. However, changes in the number of nozzles have no significant effect on changes in the angle of water spray because, at different nozzles, there is no change in pressure or nozzle diameter.

3.3. Non-Dimensional Number Analysis

For further understanding, non-dimensional number analysis was performed. The analyzed non-dimensional numbers are closely related to the droplet formation process, such as the Reynolds number, Weber number, and Froude number (Hristov, 2009).

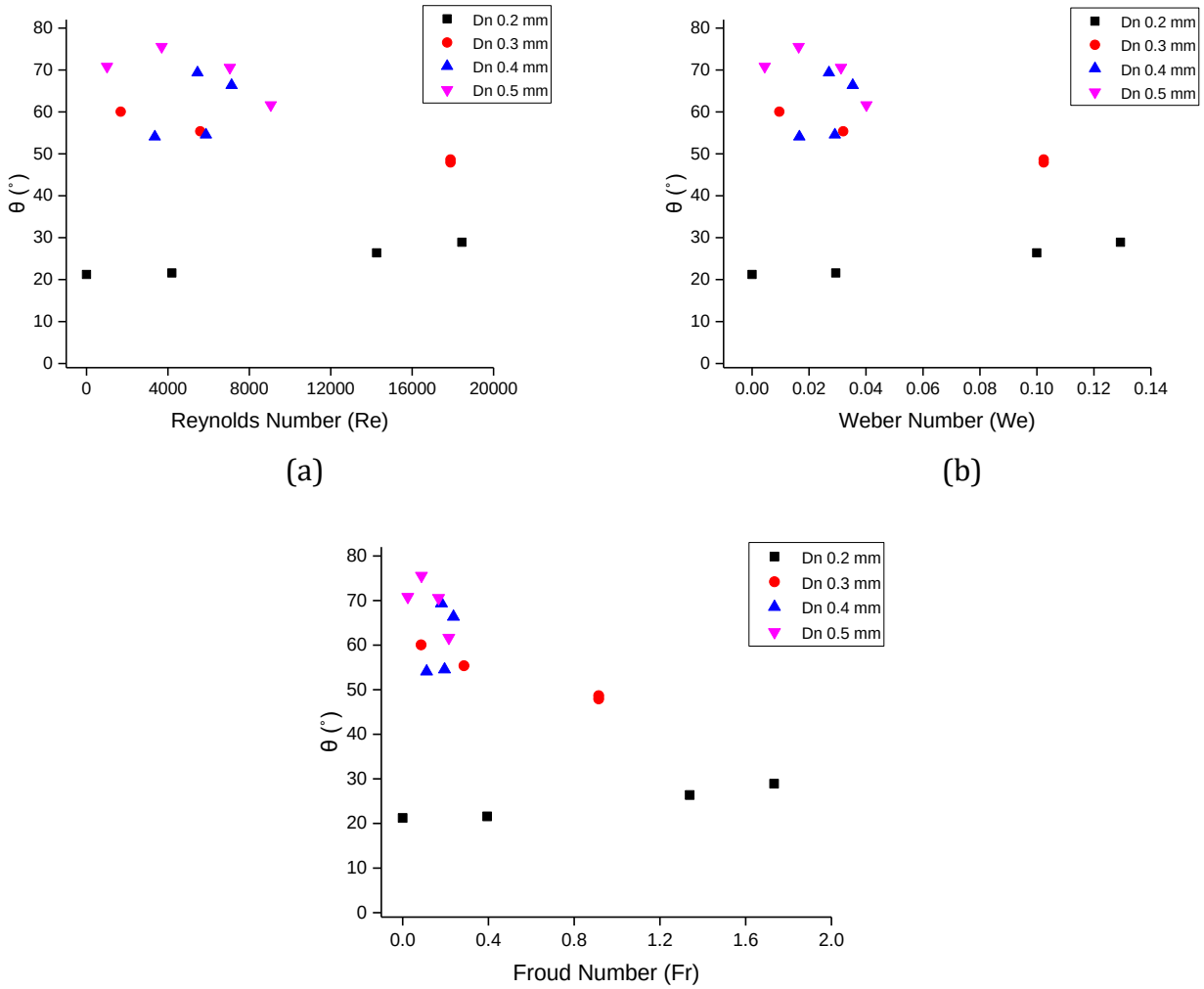

Figure 6 Graph mapping correlation between (a) Froude Number, (b) Weber Number, and (c) Reynold Number to the angle of spray (θ^0)

Figure 6a is the relationship between the Reynolds number and the spray angle. As shown in the graph in Figure 6a, Reynolds number converges in the range of 4000 to 8000 with the distribution of three flow rates having Re values below 2000 (laminar flow), two flow discharge values with values between 2000 to 4000 (transition flow), and Eleven values other discharges have Re values above 4000. The highest spray angle value of 75.55 occurs at Re 3689.2 or in transitional flow, and this condition occurs at 0.5 mm nozzle diameter and 9 bar pressure. While the largest Re value of 18446.14 occurred at a spray angle of 28.92˚ with a nozzle diameter of 0.2 mm and a pressure of 9 bar.

In Figure 6b, there is a graph showing the mapping of the relationship between the Froude number and spray angle. As inflow rate mapping, the Fr values converge in the range of 0.02 to 0.40. The graph shows fourteen values of flow discharge with a Fr value below one where the flow will move up or away from the main flow, and two flow discharge values have a Fr value above 1. For the highest spray, the angle value of 75.55˚ occurs at the Fr 0.09. This condition occurs at a nozzle diameter of 0.5 mm and a pressure of 9 bar. At the same time, the smallest Fr value is 0.02 with a spray angle of 70.82˚ at a nozzle diameter of 0.5 mm and a pressure of 8 bar.

Figure 6c shows the mapping of the Weber number to the spray angle. Based on the theory, to determine the atomization quality of the resulting spray and droplet, the largest We value is required. The We value is collected in the range of 0.0045 to 0.0401 as inflow mapping, while the largest We value occurs at the spray angle value of 28.92˚ using a nozzle diameter of 0.2 mm and a pressure of 9 bar.

The three dimensionless numbers above will affect the fluid flow characteristics and become a parameter in the formation of droplets. In this case, the pressure affects the determination of the inertial force, which requires the fluid flow velocity. In this desalination process, a good quality droplet from the atomization results is needed to get better or cleaner water quality. From the non-dimensional number, the value is used as a similarity parameter to determine droplet quality.

4. Conclusions

This study proves that pressure affects the characteristics of the spray, namely the angle of water spray at the nozzle diameter and a certain number of nozzles. The greater the pressure applied to the water stream, the greater the angle of the spray produced. The effect of nozzle diameter also gives relevance to the spray angle. Furthermore, based on the analysis of non-dimensional numbers, it was determined that the configuration of a series of two nozzles with a diameter of 0.5 mm at a pressure of 9 bar was the best water spray configuration.

Acknowledgments

This work was supported by the Ministry of Research, Technology, and Higher Education (KEMENRISTEK DIKTI) of the Republic of Indonesia with grant No: NKB-038/UN2.RST/HKP.05.00/2021.

References

Abdelkareem, M.L.E., 2019. *Dynamic Behavior and Performance of Different Types of Multi-Effect Desalination Plants*. Doctoral's Dissertation, University of Central Florida Orlando, Florida

Arunkumar, T., Jayaprakash, R., Ahsan, A., Denkenberger, D., Okundamiya, M.S., 2013. Effect Of Water and Air Flow On Concentric Tubular Solar Water Desalting System. *Applied Energy*, Volume 103, pp. 109–115

Chen, Q., Thu, K., Bui, T.D., Li, Y., Ng, K.C., Chua, K.J., 2016. Development of a Model For Spray Evaporation Based on Droplet Analysis. *Desalination*, Volume 399, pp. 69–77

Chen, Q., Li, Y., Chua, K.J., 2016. On The Thermodynamic Analysis of a Novel Low-Grade Heat Driven Desalination System. *Energy Conversion and Management*, Volume 128, pp. 145–159

Christ, A., Regenauer-Lieb, K., Chua, H.T., 2014. Thermodynamic Optimisation of Multi Effect Distillation Driven by Sensible Heat Sources. *Desalination*, Volume 336(1), pp. 160–167

Darwish, M., Mohtar, R., Elgendy, Y., Chmeissani, M., 2012. Desalting Seawater in Qatar By Renewable Energy: A Feasibility Study. *Desalination and Water Treatment*, Volume 47(1–3), pp. 279–294

El-Agouz, S.A., Abd El-Aziz, G.B., Awad, A.M., 2014. Solar Desalination System Using Spray Evaporation. *Energy,* Volume 76, pp. 276–283

El-Fiqi, A.K., Ali, N.H., El-Dessouky, H.T., Fath, H.S., El-Hefni, M.A., 2007. Flash Evaporation in A Superheated Water Liquid Jet. *Desalination*, Volume 206(1–3), pp. 311–321

Gude, V.G., 2011. Energy Consumption and Recovery in Reverse Osmosis. *Desalination and Water Treatment*, 36(1–3), pp. 239–260

He, W.F., Han, D., Yue, C., Pu, W.H., 2015. A Parametric Study of a Humidification Dehumidification (HDH) Desalination System Using Low Grade Heat Sources. *Energy Conversion and Management*, Volume 105, pp. 929–937

Hristov, J., 2010. Benchmarking of the Construct of Dimensionless Correlations Regarding Batch Bubble Columns with Suspended Solids: Performance of The Pressure Tra Form Approach. *arXiv preprint arXiv,* Volume 2010, pp. 475–483

Hwang, T.H., Moallemi, M.K., 1988. Heat Transfer of Evaporating Droplets in Low Pressure Systems. *International Communications in Heat and Mass Transfer*, Volume 15(5), pp. 635–644

Ikegami, Y., Sasaki, H., Gouda, T., Uehara, H., 2006, Experimental Study on A Spray Flash Desalination (Influence of The Direction of Injection. *Desalination*, Volume 194(1–3), pp. 81–89

Kusuma, M.H., Putra, N., Respati, R.E., 2018. A New Cascade Solar Desalination System with Integrated Thermosyphons. *International Journal of Technology*, Volume 9(2), pp. 297–306

Mayer, F.T., Fringer, O.B., 2017. An Unambiguous Definition of The Froude Number for Lee Waves In The Deep Ocean. *Journal of Fluid Mechanics*, Volume 831, pp. 1–9

Miyatake, O., Tomimura, T., Ide, Y., Fujii, T., 1981a. An Experimental Study of Spray Flash Evaporation. *Desalination*, Volume 36(2), pp. 113–128

Miyatake, O., Tomimura, T., Ide, Y., Yuda, M., Fujii, T., 1981b. Effect of Liquid Temperature on Spray Flash Evaporation. *Desalination*, Volume 37(3), pp. 351–366

Mutair, S., Ikegami, Y., 2008. Study and Enhancement of Flash Evaporation Desalination Utilizing The Ocean Thermocline And Discharged Heat. *Proceeding of World Academy of Science, Engineering and Technology*, Volume 33, pp. 473–481

Mutair, S., Ikegami, Y., 2009. Experimental Study on Flash Evaporation from Superheated Water Jets: Influencing Factors and Formulation of Correlation. *International Journal of Heat and Mass Transfer*, Volume 52(23–24), pp. 5643–5651

Nugroho, A., 2004. Uraian Umum tentang Teknologi Desalinasi (*General Description of Desalination Technology). Jurnal Pengembangan Energi Nuklir*, Volume 6(2), pp. 65–75

Rapp, B.E., 2016. *Microfluidics: Modeling, mechanics and mathematics*. Elsevier

Badan Pusat Statistik (BPS), 2020. *Statistik Air Bersih 2014-2019* (*Clean Water Statistics 2014-2019*). Badan Pusat Statistik, Indonesia

Uruba, V., 2018, On Reynolds Number Physical Interpretation. *AIP Conference Proceedings*, Vol. 2000(1), p. 020019

Utami, T.S., Arbianti, R., Manaf, B.N., 2015. Sea Water Desalination Using Debaryomyces Hansenii with Microbial Desalination Cell Technology. *International Journal of Technology*, Volume 6(7), pp. 1094–1100

Warjito, Harinaldi, Setyantono, M., 2016. Visualization of Angular Particle-Bubble Surface Interaction Using a High Speed Video Camera. *International Journal of Technology*, Volume 7(6), pp. 1045–1053

Wellmann, J., Neuhäuser, K., Behrendt, F., Lehmann, M., 2015. Modeling An Innovative Low-Temperature Desalination System With Integrated Cogeneration In A Concentrating Solar Power Plant. *Desalination and Water Treatment*, Volume 55(12), pp. 3163–3171

Zhang, S., Tao, X., Lu, J., Wang, X. and Zeng, Z., 2015. Structure Optimization And Numerical Simulation of Nozzle for High Pressure Water Jetting. *Advances in Materials Science and Engineering*, 2015(February 2016). doi: 10.1155/2015/732054